DMD Fast Forward. Published on May 3, 2017 as DOI: 10.1124/dmd.116.074823
This article has not been copyedited and formatted. The final version may differ from this version.

DMD # 74823

Comparison of methods for estimating unbound intracellular-to-medium concentration ratios in rat and human hepatocytes using statins

Takashi Yoshikado, Kota Toshimoto, Tomohisa Nakada, Kazuaki Ikejiri, Hiroyuki Kusuhara, Kazuya Maeda, and Yuichi Sugiyama

Sugiyama Laboratory, RIKEN Innovation Center, RIKEN, 1-7-22 Suehiro-cho, Tsurumi-ku, Yokohama, Kanagawa 230-0045, Japan (T.Y., K.T., Y.S.)

DMPK Research Laboratories Sohyaku, Innovative Research Division, Mitsubishi Tanabe Pharma Corporation, 2-2-50, Kawagishi, Toda-shi, Saitama 335-8505, Japan (T.N.)

Laboratory of Molecular Pharmacokinetics, Graduate School of Pharmaceutical Sciences, the University of Tokyo, 7-3-1 Hongo, Bunkyo-ku, Tokyo 113-0033, Japan (K.I., H.K., K.M.)

DMD Fast Forward. Published on May 3, 2017 as DOI: 10.1124/dmd.116.074823
This article has not been copyedited and formatted. The final version may differ from this version.

DMD # 74823

Running title: Unbound hepatocyte-to-medium concentration ratio

Corresponding author: Yuichi Sugiyama, Ph.D., Head of Sugiyama Laboratory

Address: Sugiyama Laboratory, RIKEN Innovation Center, RIKEN, 1-7-22 Suehiro-cho, Tsurumi-ku, Yokohama, Kanagawa 230-0045, Japan

Phone: +81-45-503-9211 Fax: +81-45-503-9190

E-mail: ychi.sugiyama@riken.jp

Numbers of manuscript elements:

Text pages: 36

Tables: 8

Figures: 6

Supplemental Table: 1

Supplemental Figures: 3

References: 38

Words in Abstract: 248

Words in Introduction: 613

Words in Discussion: 1475

Abbreviations: AFE, average fold error; ATP, adenosine triphosphate; BCRP, breast cancer resistance protein; CL_{int}, hepatic intrinsic clearance for metabolism and biliary excretion of unchanged drugs; CYP, cytochrome P450; C/M ratio, cell-to-medium total concentration ratio; DDI, drug–drug interaction; f_B, unbound fraction in blood; $f_{T,cell,ss}$, unbound fraction in

hepatocytes at steady state; $f_{T,homogenate}$, unbound fraction in liver homogenates; $f_{T,cell,V0}$, unbound fraction in hepatocytes based on initial uptake rate; K_i, inhibition constant; K_m, Michaelis–Menten constant; $K_{p,uu,ss}$, unbound hepatocyte-to-medium concentration ratio based on steady-state uptake; $K_{p,uu,true}$, theoretically true unbound hepatocyte-to-medium concentration ratio; $K_{p,uu,V0}$, unbound hepatocyte-to-medium concentration ratio based on initial uptake rate; $\Delta\Psi$, membrane potential; MRP, multidrug resistance-associated protein; NTCP, Na^+-taurocholate cotransporting polypeptide; OATP, organic anion transporting polypeptide; P-gp, P-glycoprotein; $PS_{inf,act}$, active uptake intrinsic clearance on sinusoidal membrane; PS_{dif}, influx intrinsic clearance by passive diffusion through sinusoidal membrane; SD, standard deviation; TPP^+, tetraphenylphosphonium; UGT, uridine 5′-diphospho-glucuronosyltransferase; V_{max}, maximum transport rate

DMD Fast Forward. Published on May 3, 2017 as DOI: 10.1124/dmd.116.074823
This article has not been copyedited and formatted. The final version may differ from this version.

Abstract

It is essential to estimate concentrations of unbound drugs inside the hepatocytes to predict hepatic clearance, efficacy, and toxicity of the drugs. The present study was undertaken to compare predictability of the unbound hepatocyte-to-medium concentration ratios ($K_{p,uu}$) by two methods based on the steady-state cell-to-medium total concentration ratios at 37°C and on ice ($K_{p,uu,ss}$) and based on their initial uptake rates ($K_{p,uu,V0}$). Poorly metabolized statins were used as test drugs because of their concentrative uptake via organic anion transporting polypeptides (OATPs). $K_{p,uu,ss}$ values of these statins provided less interexperimental variation than the $K_{p,uu,V0}$ values, because only data at longer time are required for $K_{p,uu,ss}$. $K_{p,uu,V0}$ values for pitavastatin, rosuvastatin, and pravastatin were 1.2–5.1-fold $K_{p,uu,ss}$ in rat hepatocytes; $K_{p,uu,V0}$ values in human hepatocytes also tended to be larger than corresponding $K_{p,uu,ss}$. To explain these discrepancies, theoretical values of $K_{p,uu,ss}$ and $K_{p,uu,V0}$ were compared with true $K_{p,uu}$ ($K_{p,uu,true}$) considering the inside-negative membrane potential and ionization of the drugs in hepatocytes and medium. Membrane potentials were approximately –30 mV in human hepatocytes at 37°C and almost abolished on ice. Theoretical equations considering the membrane potentials indicate that $K_{p,uu,ss}$ values for the statins are 0.85–1.2-fold $K_{p,uu,true}$, whereas $K_{p,uu,V0}$ values are 2.2–3.1-fold $K_{p,uu,true}$, depending on the ratio of the passive permeability of the ionized to nonionized forms. In conclusion, $K_{p,uu,ss}$ values of anions are similar to $K_{p,uu,true}$ when the inside-negative membrane potential is considered. This suggests that $K_{p,uu,ss}$ is preferable for estimating the concentration of unbound drugs inside the hepatocytes.

Introduction

According to the free drug hypothesis, only unbound drug is believed to interact with metabolic enzymes and pharmacological/toxicological target proteins. Knowing the intracellular unbound drug concentration is essential to estimate accurately the risk of drug–drug interactions (DDIs) involving drug-metabolizing enzymes and canalicular efflux transporters, and efficacy and toxicity of drugs when their targets are intracellular proteins. Extracellular unbound drug concentration is frequently assumed to be equivalent to the intracellular unbound concentration, especially when drugs are neutral or nonionized and freely permeable across the cytoplasmic membrane (Smith et al., 2010). However, this assumption cannot be applied to drugs whose tissue uptake is dominated by active transporters (Smith et al., 2005; Shugarts and Benet, 2009; International Transporter et al., 2010; Niemi et al., 2011; Shitara et al., 2013), where their intracellular unbound concentration of drugs could be higher than the extracellular unbound concentration. For instance, unbound concentrations of pravastatin and rosuvastatin in the rat liver are 11–16-fold (Yamazaki et al., 1993; Nezasa et al., 2003) and 15-fold higher than unbound plasma concentrations, respectively, because of organic anion transporting polypeptide (Oatp)-mediated uptake (Nezasa et al., 2003).

Methods to estimate the unbound hepatocyte-to-medium concentration ratio ($K_{p,uu}$) are needed to predict the magnitude of DDIs involving drug-metabolizing enzymes, efflux transporters, and other intrahepatic target proteins in the liver. Brown et al. investigated the impact of transporters on the inhibition constant (K_i) values of cytochrome P450 (CYP) inhibitors by comparing their inhibitory effects using rat liver microsomes and freshly isolated rat hepatocytes (Brown et al., 2010). Using the hepatocytes, K_i values of clarithromycin and enoxacin with known hepatic transporter involvement were markedly smaller than those using the microsomes, which was consistent with their high

cell-to-medium total concentration ratios (C/M ratios). The International Transporter Consortium published a review summarizing strategies to estimate intracellular drug concentrations (Chu et al., 2013). Among them, a strategy to estimate $K_{p,uu}$ based on the initial uptake rate ($K_{p,uu,V0}$) calculated using active transport clearance (V_{max}/K_m) and passive diffusion clearance at various concentrations (Yabe et al., 2011) was introduced. In addition, we have proposed an alternative strategy to estimate $K_{p,uu}$ under steady-state conditions ($K_{p,uu,ss}$), which can be calculated by dividing the C/M ratio at 37°C by that at a low temperature (on ice) or in the presence of ATP depletors, when active transport is stopped (Yamazaki et al., 1992; Shitara et al., 2013). Yamazaki et al. demonstrated that the uptake of pravastatin by rat hepatocytes was more greatly reduced at a low temperature than by ATP depletion (Yamazaki et al., 1993).

In the present study, steady-state uptake of typical Oatp/OATP substrates, pitavastatin, rosuvastatin, and pravastatin in rat and human hepatocytes, was investigated at 37°C and on ice to evaluate their $K_{p,uu,ss}$. In general, $K_{p,uu}$ can be described by the C/M ratio of drugs in hepatocytes as follows:

$$C/M \quad ratio = \frac{C_{cell}}{C_{medium}} = \frac{C_{cell,unbound} / f_T}{C_{medium,unbound} / f_B} = K_{p,uu} \cdot \frac{f_B}{f_T}, \qquad \text{(Eq. 1)}$$

where f_B is the unbound fraction of the drugs in the blood (*in vivo*) or in the incubation medium (*in vitro*), and f_T is the unbound fraction of the drugs in the hepatocytes. The unbound fraction in hepatocytes at the steady state ($f_{T,cell,ss}$) obtained using our method should be validated because intracellular binding to cytosolic proteins/cellular organelles might be altered at low temperatures. Therefore, $f_{T,cell,ss}$ were compared with the unbound fraction in liver homogenates ($f_{T,homogenate}$) measured by equilibrium dialysis using human liver samples. The $K_{p,uu,ss}$ obtained were then compared with $K_{p,uu,V0}$ in both rat and human hepatocytes. The difference between $K_{p,uu,ss}$ or $K_{p,uu,V0}$ and true $K_{p,uu}$ ($K_{p,uu,true}$) is discussed in the context

DMD Fast Forward. Published on May 3, 2017 as DOI: 10.1124/dmd.116.074823
This article has not been copyedited and formatted. The final version may differ from this version.

of theoretical equations considering the membrane potential in hepatocytes and the fraction of ionized drugs at the designated pH. Finally, a method to predict $K_{p,uu,true}$ from $K_{p,uu,ss}$ and $K_{p,uu,V0}$ obtained experimentally is proposed.

DMD Fast Forward. Published on May 3, 2017 as DOI: 10.1124/dmd.116.074823
This article has not been copyedited and formatted. The final version may differ from this version.

Materials and Methods

Chemicals. [^{3}H]Pitavastatin, [^{3}H]rosuvastatin calcium, and [^{3}H]pravastatin calcium were obtained from American Radiolabeled Chemicals (St. Louis, MO). [^{3}H]Diazepam was obtained from PerkinElmer Life Sciences (Boston, MA). Unlabeled diazepam, pitavastatin calcium, rosuvastatin calcium, and pravastatin sodium were obtained from Wako Pure Chemicals (Osaka, Japan). All other reagents and solvents were purchased from Invitrogen (Carlsbad, CA), Sigma-Aldrich (St. Louis, MO), and Wako Pure Chemicals.

Animals. Male Sprague Dawley rats were purchased from Charles River Japan (Shiga, Japan) and acclimatized for >7 days before the experiments. The rats were housed under conditions of controlled temperature and humidity with a 12-h light/dark cycle with free access to standard laboratory rodent food (CE-2; CLEA Japan, Tokyo, Japan) and water. All animal experiments were approved by the Experimental Animal Care and Use Committee of the Mitsubishi Tanabe Pharma Corporation, and conducted in accordance with the Declaration of Helsinki and the guidelines of the ethics committee.

Isolation of rat hepatocytes. Hepatocytes were isolated from male Sprague Dawley rats (7–9 weeks old) using a procedure described previously (Baur et al., 1975). Isolated hepatocytes were suspended in albumin-free Krebs–Henseleit buffer with 12.5 mM HEPES (pH 7.4), and cell viabilities were determined using a trypan blue exclusion test. Hepatocytes obtained from three independent preparations with >80% viability were used for the uptake studies described below.

Preparation of human hepatocytes. Human biological samples were obtained ethically and their research use was in accordance with the terms of informed consent. Cryopreserved

human hepatocytes from a donor (Lot Hu8075) were purchased from Life Technologies (Carlsbad, CA). Pooled cryopreserved human hepatocytes from 20 mixed-sex donors (Lot TFF) were purchased from BioreclamationIVT (Baltimore, MD). Pooled cryopreserved human hepatocytes from 50 mixed-sex donors (Lot HUE50C) were purchased from Thermo Fisher Scientific (Waltham, MA). These hepatocytes were suspended in albumin-free Krebs–Henseleit buffer with 12.5 mM HEPES (pH 7.4), and viabilities were determined using a trypan blue exclusion test. Hepatocytes obtained from three independent preparations with >80% viability were used for the uptake studies described below.

Determination of the intracellular volume of hepatocytes. The intracellular volume of rat hepatocytes (3.68 ± 1.37 μL/10^6 cells) was estimated using published methods (Supplemental Table 1A) (Baur et al., 1975; Kletzien et al., 1975; Eaton and Klaassen, 1978; Kristensen and Folke, 1984; Yamazaki et al., 1992; Miyauchi et al., 1993; Reinoso et al., 2001; Hallifax and Houston, 2006). In brief, to determine the intracellular volume of human hepatocytes, cryopreserved human hepatocytes (Lot Hu8075) were suspended in Krebs–Henseleit buffer (pH 7.4) at 6.0 × 10^6 viable cells/mL and preincubated at 37°C for 5 min. A reaction was initiated by adding an equal volume of buffer containing [^{3}H]water and [^{14}C]dextran at final concentrations of 2.5 μCi/mL and 0.5 μCi/mL, respectively. After incubation at 37°C for 10 min, during which the distribution of [^{3}H]water and [^{14}C]dextran reached a steady state, aliquots were removed and added to a narrow tube containing silicone–mineral oil (density: 1.015, Sigma-Aldrich) over aqueous 2 M sodium hydroxide, followed by centrifugation through the silicone–mineral oil layer to separate the cells from the medium. After the basic bottom layer was neutralized with 2 M hydrochloric acid, radioactivities in both cells and medium were determined using a Tri-Carb liquid scintillation counter (PerkinElmer, Shelton, CT). Thereby, the intracellular volume of human hepatocytes was estimated to be 2.28 ± 0.33

μL/10^6 cells (Supplemental Table 1B).

Determination of $K_{p,uu,ss}$ and $f_{T,cell,ss}$ in rat and human hepatocytes based on steady-state uptake. To determine the incubation time for steady-state uptake into hepatocytes, transport studies were performed by an oil-spin method (Iga et al., 1979) using suspended hepatocytes. Hepatocytes were suspended in Krebs–Henseleit buffer (pH 7.4) at 2.0×10^6 viable cells/mL and preincubated at 37°C for 5 min. A reaction was initiated by adding an equal volume of buffer containing each drug (pitavastatin, rosuvastatin, pravastatin, or diazepam previously used as a neutral drug with high membrane permeability for evaluating the uptake into isolated rat hepatocytes (Ichikawa et al., 1992)) at 1 μM. After incubation at 37°C for 0.5, 2, 5, 15, and 30 min (rat hepatocytes), 0.5, 5, 15, 30, and 60 min (human hepatocytes, Lot Hu8075), or 0.5, 1.5, 30, and 60 min (human hepatocytes, Lot TFF), aliquots were removed and added to a narrow tube containing silicone–mineral oil over aqueous 2 M sodium hydroxide and centrifuged through the silicone–mineral oil layer to separate the cells from the medium. To provide low temperature values, the uptake studies were performed on ice. After the basic bottom layer was neutralized with 2 M hydrochloric acid, radioactivity in both cells and medium were measured using the liquid scintillation counter.

The unbound hepatocyte-to-medium concentration ratio ($K_{p,uu}$) based on the steady-state uptake ratio at 37°C and on ice ($K_{p,uu,ss}$), and the unbound fraction in hepatocytes based on the steady-state uptake ($f_{T,cell,ss}$) were defined as described in Equations 2 and 3, respectively, based on the C/M ratio at 37°C and on ice. A part of the method to obtain $f_{T,cell,ss}$ was reported previously (Yoshikado et al., 2016).

DMD Fast Forward. Published on May 3, 2017 as DOI: 10.1124/dmd.116.074823
This article has not been copyedited and formatted. The final version may differ from this version.

$$K_{p,uu,ss} = \frac{C/M\ ratio_{37℃}}{C/M\ ratio_{on\ ice}} = \frac{C_{cell,37℃}/C_{medium,37℃}}{C_{cell,on\ ice}/C_{medium,on\ ice}}$$

$$= \frac{C_{cell,unbound,37℃}/C_{medium,37℃}/f_{T,cell,37℃}}{C_{cell,unbound,on\ ice}/C_{medium,on\ ice}/f_{T,cell,on\ ice}}$$

$$= \frac{C_{cell,unbound,37℃}}{C_{medium,37℃}} \quad \text{(Eq. 2)}$$

$$f_{T,cell,ss} = \frac{C_{cell,unbound,on\ ice}}{C_{medium,on\ ice}} \cdot \frac{C_{medium,on\ ice}}{C_{cell,on\ ice}}$$

$$= \frac{1}{C/M\ ratio_{on\ ice}} \quad \text{(Eq. 3)}$$

The following assumptions were made in calculating $K_{p,uu,ss}$ and $f_{T,cell,ss}$ using Equations 2 and 3: the active uptake in hepatocytes is abolished on ice (i.e., $C_{cell,unbound,on\ ice}$ is equal to $C_{medium,on\ ice}$), and $f_{T,cell,ss}$ is independent of temperature (i.e., $f_{T,cell,ss,on\ ice}$ is equal to $f_{T,cell,ss,37°C}$).

Determination of $K_{p,uu,V0}$, $f_{T,cell,V0}$, and other kinetic parameters in rat and human hepatocytes based on initial uptake rate. To evaluate the initial uptake rate in pooled human hepatocytes, hepatocytes were preincubated for 5 min and then incubated for 0.5–1.5 or 0.5–2 min, as shown in the transport studies described above.

The uptake clearance by hepatocytes (CL_{uptake}) was determined by the slope of the plot of C/M ratio versus time, and the initial uptake rate (*v*) was calculated by multiplying CL_{uptake} with the initial substrate concentration.

According to a method reported previously (Yabe et al., 2011), *v* can be calculated using Equation 4:

DMD Fast Forward. Published on May 3, 2017 as DOI: 10.1124/dmd.116.074823
This article has not been copyedited and formatted. The final version may differ from this version.

$$v = \frac{V_{max} \cdot S}{K_m + S} + PS_{dif} \cdot S \,, \qquad \text{(Eq. 4)}$$

where V_{max} is the maximum uptake rate, K_m is the Michaelis constant, PS_{dif} is the passive diffusion clearance, and S is the substrate concentration in the medium. These kinetic parameters were optimized by fitting the equation to observed data using Phoenix WinNonlin version 6.3 (Pharsight Certara, St. Louis, MO). Because CL_{uptake} consists of active uptake clearance (PS_{act}) and passive diffusion clearance (PS_{dif}), assuming that PS_{dif} for the cellular uptake is equal to that for the efflux, $K_{p,uu}$ and $f_{T,cell}$ based on initial uptake rate ($K_{p,uu,V0}$, $f_{T,cell,V0}$) can be calculated using Equations 5 and 6 (Yabe et al., 2011):

$$K_{p,uu,V0} = \frac{PS_{act} + PS_{dif}}{PS_{dif}} \,, \qquad \text{(Eq. 5)}$$

$$f_{T,cell,V0} = \frac{K_{p,uu,V0}}{\text{C/M ratio}_{37°C}} \,, \qquad \text{(Eq. 6)}$$

where the C/M $ratio_{37°C}$ in rat hepatocytes was obtained at 30 min, and that in human hepatocytes was obtained at 60 min.

Determination of the unbound fraction in human liver homogenates ($f_{T,homogenate}$) using equilibrium dialysis. Human liver samples were obtained from the Human & Animal Bridging (HAB) Research Organization (Tokyo, Japan) with approval of the Ethics Committees of The University of Tokyo and HAB Research Organization. Three lots of liver samples were pooled and homogenized in 66.7 mM isotonic phosphate buffer at 1:3 (w/v) producing 25% homogenates. By diluting these homogenates, 12.5% and 6.25% homogenates were also prepared. Diazepam, pitavastatin, pravastatin, and rosuvastatin (final concentrations: 0.2 μM) were added to the compartment containing homogenates in a Rapid Equilibrium Dialysis plate (Thermo Fisher Scientific) and incubated for 12 h at 37°C, or on

ice.

Calculation of the ratio of passive diffusion influx clearance of ionized drug to that of nonionized drug (λ) based on the pH-dependent permeability examined in Caco-2 cells. Caco-2 cells were obtained from American Type Culture Collection (Rockville, MD). Cells (passages 28–40) were cultivated as previously described (Neuhoff et al., 2003) with some modifications. Briefly, Caco-2 cells were seeded onto a Millicell-96 Cell Culture Insert Plate (polycarbonate 0.4 μm; Millipore, MA) at 2.5×10^5 cells/well and the culture medium was changed every second day. On day 10, transport experiments were performed; the incubation medium was HBSS buffered with either 20 mM MES (pH = 5.5, 6.0, and 6.5), or 20 mM HEPES (pH = 7.4). Before the experiments, the apical side of the Caco-2 cell monolayer was washed four times with HBSS at the corresponding pHs (5.5, 6.0, 6.5, and 7.4). Then, both apical and basal sides of the monolayer were preincubated for 10 min at 37°C in the presence of rifamycin SV (100 μM), cyclosporin A (10 μM), and Ko143 (10 μM) as OATP2B1, P-glycoprotein (P-gp), and breast cancer resistance protein (BCRP) inhibitors, respectively, at corresponding pHs (5.5, 6.0, 6.5, and 7.4 for the apical side, and 7.4 for the basal side). Subsequently, the monolayer was incubated for 10, 30, 60, and 90 min at 37°C in the presence of each radiolabeled statin (10 μM, apical side only) and the inhibitors (both sides). Lucifer yellow (300 μM) was used as a paracellular marker to examine the integrity of the monolayer. The radioactivity on the basal side was determined using a liquid scintillation counter.

The passive diffusion influx clearance ($PS_{dif,inf}$) is expressed as follows:

DMD Fast Forward. Published on May 3, 2017 as DOI: 10.1124/dmd.116.074823
This article has not been copyedited and formatted. The final version may differ from this version.

$$PS_{dif,inf} = f_{o,ion} \cdot PS_{dif,inf,ion} + f_{o,uion} \cdot PS_{dif,inf,uion}$$

(Eq. 7)

where the subscripts ion and uion represent the ionized and unionized (nonionized) form of a drug, respectively, and $f_{o,ion}$ and $f_{o,uion}$ are fractions of ionized and nonionized drug outside the cells, respectively. Subsequently, λ was defined as the ratio of passive diffusion influx clearance of the ionized drug to that of the nonionized drug as follows:

$$\lambda = \frac{PS_{dif,\mathrm{inf},ion}}{PS_{dif,\mathrm{inf},uion}}. \quad \text{(Eq. 8)}$$

It is assumed that the λ value is not changed by temperature: the effect of low temperature on $PS_{dif,inf,ion}$ is assumed to be the same as that on $PS_{dif,inf,uion}$, although these passive diffusion clearances should be affected by the change in membrane fluidity at low temperature (Kanduser et al., 2008). A part of the method to obtain λ was reported previously (Yoshikado et al., 2016). Using λ, Equation 7 can be converted as follows:

$$\begin{aligned} PS_{dif,\mathrm{inf}} &= (1 - f_{o,uion}) \cdot PS_{dif,\mathrm{inf},ion} + f_{o,uion} \cdot PS_{dif,\mathrm{inf},uion} \\ &= \left(\lambda \cdot (1 - f_{o,uion}) + f_{o,uion}\right) \cdot PS_{dif,\mathrm{inf},uion} \\ &= \left(\lambda + (1-\lambda) \cdot f_{o,uion}\right) \cdot PS_{dif,\mathrm{inf},uion} \\ &= \left(\lambda + \frac{(1-\lambda)}{10^{pH-pKa}+1}\right) \cdot PS_{dif,\mathrm{inf},uion} \end{aligned} \quad \text{(Eq. 9)}$$

The $f_{o,ion}$ and $f_{o,uion}$ for each statin were estimated using the pH of the medium (7.4) and pKa of the drug obtained from the manufacturer's Interview Forms, based on the Henderson–Hasselbalch equation (Table 1). Then, λ and $PS_{dif,inf,uion}$ in Caco-2 cells were optimized by fitting Equation 9 to the pH-dependent membrane permeation of statins (Supplemental Figure 1). Phoenix WinNonlin software version 6.3 (Pharsight Certara) was used to optimize the parameters. The obtained λ values for pitavastatin, rosuvastatin, and pravastatin are shown in

DMD Fast Forward. Published on May 3, 2017 as DOI: 10.1124/dmd.116.074823
This article has not been copyedited and formatted. The final version may differ from this version.

Table 1.

Measurement of the membrane potential using a lipophilic cation. Tetraphenylphosphonium (TPP^+) is a lipophilic cation that has been used as a probe to determine the membrane potential ($\Delta\Psi$). Saito et al. suggested a method to evaluate the $\Delta\Psi$ with TPP^+ correcting for its binding to intracellular constituents and its significant accumulation in mitochondria (Saito et al., 1992). By measuring the C/M ratio of TPP^+, $\Delta\Psi$ is calculated as described in Equation 10 (Saito et al., 1992):

$$\Delta\Psi = -(RT/F)\ln\left(\frac{C/M_{phys}ratio}{C/M_{abol}ratio}\right), \quad \text{(Eq. 10)}$$

where R, T, and F are the gas constant, absolute temperature, and Faraday constant, respectively. C/M_{phys} and C/M_{abol} are the C/M under physiological conditions and when the $\Delta\Psi$ is abolished, respectively. The selective abolition of $\Delta\Psi$ can be achieved by rendering the cytoplasmic membrane permeable with 20 μM of amphotericin B (Saito et al., 1992). To measure the C/M ratio of TPP^+, transport studies were performed using an oil-spin method (Iga et al., 1979) with cryopreserved human hepatocytes (Lot HUE50C). Hepatocytes were suspended in Krebs–Henseleit buffer (pH 7.4) at 2.0×10^6 viable cells/mL and preincubated at 37°C for 5 min. The reaction was initiated by adding an equal volume of buffer containing TPP^+ (final: 3 μM) and amphotericin B (final: 20 μM). After incubation at 37°C for 0.5, 15, 30, and 60 min, aliquots were removed and added to a narrow tube containing silicone–mineral oil over a 2.5 M ammonium acetate, and then centrifuged to separate the cells from the medium. To examine the effect of low temperature on $\Delta\Psi$, uptake studies were also performed on ice. The concentrations of TPP^+ in the cells and the medium were determined using an LC-MS/MS system equipped with a Nexera UHPLC and a LCMS-8050 triple

quadrupole liquid chromatograph mass spectrometer (Shimadzu, Kyoto, Japan). A Kinetex C18 column (2.6 μm, 3 mm × 100 mm; Phenomenex, Torrance, CA) was used, and UHPLC was conducted under gradient mobile-phase conditions with a mixture of 0.1% formic acid in water and 0.1% formic acid in acetonitrile as solvents (0.3 mL/min; 0–0.5 min 95:5 v/v, 0.5–3.5 min 95:5 to 15:85 v/v, 3.5–5 min 15:85 v/v, 5–5.5 min 15:85 to 5:95 v/v, 5.5–6 min 5:95 v/v, 6–6.1 min 5:95 to 95:5 v/v, and 6.1–6.5 min 95:5 v/v). The UHPLC eluent was introduced into the MS in positive ESI mode. TPP^+ was quantified in multiple reaction monitoring (MRM) mode (339.10 > 183.10; Q1 prebias: –30.0 V, CE: –54.0, Q3 prebias: –17.0 V), in which chlorpropamide was used as an internal standard (277.20 > 111.05; Q1 prebias: –18.0 V, CE: –32.0, Q3 prebias: –20.0 V).

Evaluation of the correlation between $K_{p,uu}$ values examined by the two different methods. To quantitatively evaluate the correlation between $K_{p,uu,ss}$ and $K_{p,uu,V0}$, commonly employed accuracy test criteria, the average fold errors (AFE), were calculated as shown in Equation 11.

$$AFE = 10^{\frac{\sum_{i=1}^{n}\left|\log\frac{K_{p,uu,V0}}{K_{p,uu,ss}}\right|}{n}} \qquad \text{(Eq. 11)}$$

Results

Determination of $K_{p,uu,ss}$ and $f_{T,cell,ss}$ in rat hepatocytes. The time-dependent uptake of diazepam (a lipophilic neutral compound) and pitavastatin, rosuvastatin, and pravastatin (substrates of hepatic OATPs) in rat hepatocytes was monitored. The uptake of diazepam in rat hepatocytes reached a steady state instantaneously because of its high permeability, whereas the uptake of pitavastatin, rosuvastatin, and pravastatin gradually increased over time and reached the steady state within 30 min (Fig. 1). On ice, C/M ratios of pitavastatin, rosuvastatin, and pravastatin were significantly smaller than the ratios at 37°C, while that for diazepam was not different from that at 37°C (Table 2). The $K_{p,uu,ss}$ for diazepam was 0.85 and the values for pitavastatin, rosuvastatin, and pravastatin were ca. 11, 13, and 6.7, respectively (Table 2), confirming that these statins were concentrated in the hepatocytes by an active transport system. The obtained $f_{T,cell,ss}$ values for pitavastatin, rosuvastatin, and pravastatin were ca. 0.038, 0.15, and 0.60, respectively.

Determination of $K_{p,uu,V0}$ and $f_{T,cell,V0}$ in rat hepatocytes. Subsequently, based on a method reported previously (Yabe et al., 2011), the kinetic parameters (V_{max}, K_m, and PS_{dif}) for pitavastatin, rosuvastatin, and pravastatin were determined by fitting Equation 4 to their initial uptake rate. The results are shown in Eadie–Hofstee plots (Supplemental Figure 2). The obtained $K_{p,uu,V0}$ values for pitavastatin, rosuvastatin, and pravastatin were ca. 56, 51, and 8.6, respectively (Table 3). The calculated $f_{T,cell,V0}$ for pitavastatin, rosuvastatin, and pravastatin were ca. 0.17, 0.65, and 0.69, respectively.

Determination of $K_{p,uu,ss}$ and $f_{T,cell,ss}$ in human hepatocytes. We investigated the time-dependent uptake of diazepam, pitavastatin, rosuvastatin, and pravastatin by human hepatocytes prepared from single donor (Lot Hu8075) (Fig. 2A–D) and pooled human

hepatocytes from 20 mixed-sex donors (Lot TFF) (Fig. 2E–H). The uptake of all these statins increased over time and reached a steady state within 60 min, whereas that of diazepam reached a peak instantaneously. On ice, the C/M ratios for pitavastatin, rosuvastatin, and pravastatin were reduced, while that for diazepam was not dependent on temperature (Table 4). While the $K_{p,uu,ss}$ for diazepam was ca. 1 (1.2 and 0.41), the values were 13 and 6.9 for pitavastatin, 12 and 6.4 for rosuvastatin, and 2.0 and 1.3 for pravastatin in cells from Lot Hu8075 and Lot TFF, respectively (Table 4). The obtained $f_{T,cell,ss}$ values were ca. 0.028 and 0.046 for pitavastatin, 0.22 and 0.23 for rosuvastatin, and 0.55 and 0.48 for pravastatin in cells from Lot Hu8075 and Lot TFF, respectively.

Determination of $K_{p,uu,V0}$ and $f_{T,cell,V0}$ in human hepatocytes. Based on a method reported previously (Yabe et al., 2011), the kinetic parameters (V_{max}, K_m, and PS_{dif}) for pitavastatin and rosuvastatin were determined by fitting Equation 4 to their initial uptake rate by cells from Lot Hu8075 (Supplemental Figure 3A, B) and Lot TFF (Supplemental Figure 3D, E); the kinetic parameters of pravastatin could be determined in cells from Lot Hu8075 (Supplemental Figure 3C), but not from Lot TFF, because a saturation of the uptake of pravastatin was not observed clearly within the concentration range of 0.5–300 μM.

Calculated $K_{p,uu,V0}$ values were ca. 220 and 20 for pitavastatin, 200 and 3.5 for rosuvastatin in cells from Lot Hu8075 and Lot TFF, respectively, and 55 for pravastatin in cells from Lot Hu8075 (Table 5), which were higher in cells from Lot Hu8075 than from Lot TFF. Calculated $f_{T,cell,V0}$ values were ca. 0.47 and 0.13 for pitavastatin, 3.8 and 0.13 for rosuvastatin in cells from Lot Hu8075 and Lot TFF, respectively, and 15 for pravastatin in cells from Lot Hu8075, although $f_{T,cell}$ should theoretically be less than 1. Thus, the values of $K_{p,uu,V0}$ and $f_{T,cell,V0}$ exhibited greater differences between lots.

DMD Fast Forward. Published on May 3, 2017 as DOI: 10.1124/dmd.116.074823
This article has not been copyedited and formatted. The final version may differ from this version.

Comparison of $K_{p,uu}$ and $f_{T,cell}$ obtained by different methods. In rat hepatocytes, $K_{p,uu,V0}$ values for pitavastatin, rosuvastatin, and pravastatin were respectively 5.1, 5.1, and 1.2 times those for $K_{p,uu,ss}$ (Fig. 3A). By contrast, in human hepatocytes (Lot Hu8075), $K_{p,uu,V0}$ values for pitavastatin, rosuvastatin, and pravastatin were respectively 16, 17, and 43 times those for $K_{p,uu,ss}$ (Fig. 3B). The differences between $K_{p,uu,V0}$ and $K_{p,uu,ss}$ in human hepatocytes from Lot TFF were smaller than those in Lot Hu8075: $K_{p,uu,V0}$ values for pitavastatin and rosuvastatin were respectively 2.9 and 0.55 times those for $K_{p,uu,ss}$ in cells from Lot TFF (Fig. 3B).

The $f_{T,cell,V0}$ values tended to be higher than $f_{T,cell,ss}$ in both rat (Fig. 3C) and human hepatocytes (Fig. 3D), except for rosuvastatin in human hepatocytes (Lot TFF). Both $K_{p,uu,V0}$ and $f_{T,cell,V0}$ values thus exhibited quite larger interlot and interexperimental variabilities compared with $K_{p,uu,ss}$ and $f_{T,cell,ss}$ values (comparison between Table 2 and 3 for rat, Table 4 and 5 for human).

Comparison of $f_{T,cell}$ with the measured unbound fraction in human liver homogenates. For diazepam, pitavastatin, rosuvastatin, and pravastatin, the measured unbound fractions in human liver homogenates ($f_{T,homogenate}$) were measured using equilibrium dialysis (Table 6). The $f_{T,homogenate}$ values for these drugs obtained at 37°C ($f_{T,homogenate,37°C}$) were close to those obtained on ice ($f_{T,homogenate,on\ ice}$). Moreover, the $f_{T,homogenate,on\ ice}$ values for pitavastatin and rosuvastatin were comparable to those for $f_{T,cell,ss}$ (Table 4); the difference between $f_{T,homogenate,on\ ice}$ and $f_{T,cell,ss}$ for pravastatin was within 3-fold, while there was a larger discrepancy between $f_{T,homogenate,on\ ice}$ and $f_{T,cell,ss}$ for diazepam.

Measurement of the membrane potential (ΔΨ) using TPP^+. To evaluate whether ΔΨ might affect the ratio of $PS_{dif,inf}/PS_{dif,eff}$ and accordingly, $K_{p,uu}$, the time-dependent uptake of TPP^+ was examined in human hepatocytes under physiological conditions and with

DMD Fast Forward. Published on May 3, 2017 as DOI: 10.1124/dmd.116.074823
This article has not been copyedited and formatted. The final version may differ from this version.

amphotericin B, which is reported to abolish ΔΨ specifically by 10 min incubation with isolated rat hepatocytes (Saito et al., 1992). The C/M ratio of TPP^+ gradually increased over time and reached the steady state between 30 and 60 min (Fig. 4). On ice, the C/M ratio of TPP^+ was significantly smaller than that at 37°C. In addition, in the presence of amphotericin B, the C/M ratio of TPP^+ was decreased significantly at 37°C compared with the condition without amphotericin B, while the C/M ratio on ice was not significantly changed with amphotericin B (Fig. 4). The C/M ratio (37°C) in the presence of amphotericin B at 60 min was lower than that at 30 min, suggesting some additional effects of amphotericin B (i.e., cytotoxicity) other than the loss of the ΔΨ. Therefore, based on the obtained data at 30 min and Equation 10, ΔΨ values were calculated to be ca. –30 mV at 37°C and 5 mV on ice (Table 7).

Using Φ (= exp(z·F·ΔΨ/R/T)) calculated from ΔΨ (Equation S5) and physicochemical parameters calculated for statins (Table 1), theoretical values of $K_{p,uu,true}$, $K_{p,uu,V0}$, and $K_{p,uu,ss}$ were calculated by Equations S6, S8, and S11, respectively (Table 8).

Furthermore, we aimed to understand better the quantitative relationship between $K_{p,uu,true}$ and experimentally obtained $K_{p,uu,ss}$ and $K_{p,uu,V0}$ for statins based on theoretical equations that consider the inside-negative membrane potential. Using ΔΨ (Table 7) and several physicochemical parameters of statins (Table 1), the ratios of $K_{p,uu,V0}/K_{p,uu,true}$ and $K_{p,uu,ss}/K_{p,uu,true}$ ($R_{V0/true}$ or $R_{ss/true}$) can be described as follows:

$$R_{V0/true} = {K_{p,uu,V0}}\Big/{K_{p,uu,true}} = \frac{\Phi \cdot \lambda \cdot f_{i,ion} + f_{i,uion}}{\lambda \cdot f_{o,ion} + f_{o,uion}} \quad \text{(Eq. 12)}$$

$$R_{ss/true} = {K_{p,uu,ss}}\Big/{K_{p,uu,true}} = \frac{\lambda \cdot f_{i,ion} + f_{i,uion}}{\lambda \cdot f_{o,ion} + f_{o,uion}} \quad \text{(Eq. 13)}$$

DMD Fast Forward. Published on May 3, 2017 as DOI: 10.1124/dmd.116.074823
This article has not been copyedited and formatted. The final version may differ from this version.

where $f_{i,ion}$ and $f_{i,uion}$ are fractions of the ionized and nonionized forms of the drug in hepatocytes, respectively, with the use of intracellular pH (7.2) and pKa. $R_{V0/true}$ was calculated to be 2.2–3.1 for statins, whereas $R_{ss/true}$ was 0.85–1.2 (Table 8). Figure 5 also shows that simulated $R_{ss/true}$ was closer to 1 than $R_{V0/true}$ when λ values for pitavastatin, rosuvastatin, and pravastatin were ca. 0.028, 0.011, and 0.19, respectively (Table 1). Furthermore, experimentally obtained $K_{p,uu,V0}$ and $K_{p,uu,ss}$ for statins were corrected using the calculated $R_{V0/true}$ and $R_{ss/true}$ values (Table 8) and Equations 14 and 15:

$$K_{p,uu,V0,corrected} = {K_{p,uu,V0}}/{R_{V0/true}} \quad \text{(Eq. 14)}$$

$$K_{p,uu,ss,corrected} = {K_{p,uu,ss}}/{R_{ss/true}} \quad \text{(Eq. 15)}$$

$K_{p,uu,V0,corrected}$ in rat hepatocytes approached $K_{p,uu,ss,corrected}$ (Fig. 6A) compared with uncorrected $K_{p,uu,V0}$ vs. $K_{p,uu,ss}$ (Fig. 3A): the calculated AFE are 7.6 in Figure3A and 4.4 in Figure 6A. Similarly, $K_{p,uu,V0,corrected}$ in human hepatocytes approached corrected $K_{p,uu,ss,corrected}$ (Fig. 3B and Fig. 6B): the calculated WSSs are 132 in Figure 3B and 41 in Figure 6B. However, $K_{p,uu,V0,corrected}$ in Lot Hu8075, a single donor lot selected because of its relatively high uptake ability, remained larger than $K_{p,uu,ss,corrected}$.

DMD Fast Forward. Published on May 3, 2017 as DOI: 10.1124/dmd.116.074823
This article has not been copyedited and formatted. The final version may differ from this version.

Discussion

We previously proposed a method to estimate $K_{p,uu,ss}$ for anions in hepatocytes based on their steady-state C/M ratio at 37°C and the C/M ratio after suppressing active transport (Yamazaki et al., 1992; Shitara et al., 2013). Another method reported by Yabe et al. (11) is to estimate $K_{p,uu,V0}$ based on initial uptake rates at various concentrations (Yabe et al., 2011). $K_{p,uu,ss}$ values for pitavastatin, rosuvastatin, and pravastatin in rat and human hepatocytes, which were obtained with less interexperimental variation compared with $K_{p,uu,V0}$ values in this study, tended to be smaller than the corresponding $K_{p,uu,V0}$ values (Fig. 3A, B). Considering the measured inside-negative membrane potential (Table 7) and subsequent asymmetrical diffusional clearance for influx and efflux, $K_{p,uu,V0,corrected}$ in rat and human hepatocytes approached $K_{p,uu,ss,corrected}$ (Fig. 6A, B).

There exists a practical advantage of the method to obtain the $K_{p,uu,ss}$ value over the method to obtain the $K_{p,uu,V0}$ value. Interlot and interexperimental variabilities are much less for $K_{p,uu,ss}$ than for $K_{p,uu,V0}$ (Tables 2-5), because uptake data at longer time (e.g., 30-60 min, almost at steady state) are enough to obtain $K_{p,uu,ss}$, while initial uptake rates (e.g., 0.5-1.5 or 0.5-2.0 min) are needed for $K_{p,uu,V0}$ and such a method requires quite accurate techniques for rapid samplings.

In the extended clearance concept, $K_{p,uu,true}$ is described as in Equation 16 (Shitara et al., 2013):

$$K_{p,uu,true} = \frac{PS_{act,inf} + PS_{dif,inf}}{PS_{act,eff} + PS_{dif,eff} + CL_{int,met} + CL_{int,bile}} \quad , \qquad \text{(Eq. 16)}$$

where $PS_{act,inf}$, $PS_{act,eff}$, $CL_{int,met}$, and $CL_{int,bile}$ represent the active influx clearance, the active efflux clearance, the intrinsic clearance for metabolism, and the intrinsic clearance for biliary excretion in an unchanged form, respectively. Based on Equation 16, a number of explanations can be considered for why $K_{p,uu,V0}$ values for pitavastatin, rosuvastatin, and

DMD Fast Forward. Published on May 3, 2017 as DOI: 10.1124/dmd.116.074823
This article has not been copyedited and formatted. The final version may differ from this version.

pravastatin tended to be larger than $K_{p,uu,ss}$ in both rat and human hepatocytes (Fig. 3A, B).

(i) As $PS_{act,inf}$ is estimated by initial uptake rate for the calculation for $K_{p,uu,v0}$, it may include not only active transport, but also facilitated diffusion, which is also transporter mediated, but not by active (concentrated) transport. Thus, in this case, $K_{p,uu,V0}$ can be larger than $K_{p,uu,ss}$. However, in the case of statins, hepatic OATPs are thought to be major uptake transporters, and the impact of facilitated diffusion on their overall uptake may be negligible.

(ii) The existence of nonnegligible metabolism during the measurement of steady-state uptake (30–60 min) of a drug may lead to smaller $K_{p,uu,ss}$ than $K_{p,uu,V0}$ values, because metabolism might be negligible during short incubation times (~2 min) for the measurement of initial uptake rates. Considering that pitavastatin, rosuvastatin, and pravastatin are generally classified as statins metabolized poorly in human (Shitara and Sugiyama, 2006), it is unlikely that metabolism accounts for the overestimation of $K_{p,uu,V0}$. However, a recent report suggested that pitavastatin undergoes lactonization by uridine 5′-diphospho-glucuronosyltransferases (UGTs) more extensively than other statins (Schirris et al., 2015), which may explain, at least in part, the overestimation of $K_{p,uu,V0}$ compared with $K_{p,uu,ss}$ (Fig. 3A, B). In addition, pentenoic acid derivative was reported to be the major metabolite of rosuvastatin in rats (Nezasa et al., 2002; He et al., 2014). In our experiments using rat hepatocytes, the remained amount of rosuvastatin after the 30 min-incubation was 87% of the initial amount, whereas little loss of rosuvastatin was observed after the 60 min-incubation in human hepatocytes. Therefore, the contribution of metabolism to the elimination of rosuvastatin in rats might be larger than that in humans, and the metabolism of rosuvastatin in rat hepatocytes might only slightly influence the estimation of its $K_{p,uu,ss}$.

(iii) $PS_{act,eff}$ and $CL_{int,bile}$ cannot be fully estimated by the short-term uptake of drugs. Thus, if a drug is a substrate of basolateral/apical efflux transporters, $K_{p,uu,V0}$ may be overestimated. The expression of apical efflux transporters (P-gp, multidrug

resistance-associated protein 2 (MRP2) and BCRP) and basolateral efflux transporters (MRP3 and MRP4) was partly retained in cryopreserved human hepatocytes compared with fresh liver biopsies (Lundquist et al., 2014), which might contribute, at least in part, to the drug efflux from hepatocytes and lead to a discrepancy between $K_{p,uu,V0}$ and $K_{p,uu,ss}$.

(iv) In most work, $PS_{dif,inf}$ and $PS_{dif,eff}$ are conventionally assumed to be equal for kinetic consideration of the cellular transport (Yabe et al., 2011), although $PS_{dif,eff}$ might be larger than $PS_{dif,inf}$ in the case of anions because of the inside-negative $\Delta\Psi$ in normal cells. We calculated $K_{p,uu,ss}$ by taking asymmetrical PS_{dif} into consideration with the assumption that $\Delta\Psi$ is almost abolished on ice, as we confirmed experimentally (Table 7). Conversely, to calculate $K_{p,uu,V0}$, $PS_{dif,eff}$ is set to be the same as $PS_{dif,inf}$, as shown in Equation S8. Therefore, theoretically, $K_{p,uu,V0}$ should be larger than $K_{p,uu,ss}$ in the case of anions, which might mostly explain the observed discrepancy between $K_{p,uu,ss}$ and $K_{p,uu,V0}$.

In this study, two assumptions were made. First, that $f_{T,cell,ss}$ is not affected by temperature; second, that $\Delta\Psi$ is abolished on ice. To investigate the first assumption, we sought to evaluate whether $f_{T,cell,ss}$ was largely dependent on temperature, as mentioned in previous reports (Sugano et al., 2010; Shitara et al., 2013). We found that values for $f_{T,homogenate,on\ ice}$ were comparable with those for $f_{T,homogenate,37°C}$ (Table 6), which supports the first assumption, at least for the statins tested. In addition, $f_{T,cell,ss}$ for rosuvastatin and pitavastatin measured by equilibrium dialysis were similar to $f_{T,homogenate}$, whereas $f_{T,cell,ss}$ for pravastatin was larger than $f_{T,homogenate}$ (Tables 4 and 6), although the mechanism behind this has not yet been clarified. By contrast, $f_{T,cell,V0}$ for rosuvastatin and pravastatin in human hepatocytes exceeded 1 with large standard deviations (Table 5), suggesting that it might be difficult to obtain reliable values for $f_{T,cell}$ based on the rate of initial uptake. Indeed, Yabe et al. estimated $f_{T,cell,V0}$ for some drugs including pravastatin, not by Equation 6, but by using *in silico* prediction with logD to obtain reasonable values for $f_{T,cell,V0}$ (Yabe et al., 2011).

DMD Fast Forward. Published on May 3, 2017 as DOI: 10.1124/dmd.116.074823
This article has not been copyedited and formatted. The final version may differ from this version.

The second assumption was investigated using TPP^+ uptake studies with and without amphotericin B in human hepatocytes (Fig. 4) according to a method reported previously (Saito et al., 1992). Calculated $\Delta\Psi$ at 37°C was similar to reported values (–35 to –39 mV) obtained in isolated rodent hepatocytes (Bradford et al., 1985; Edmondson et al., 1985; Fitz and Scharschmidt, 1987; Wondergem and Castillo, 1988; Weinman et al., 1989), and $\Delta\Psi$ was almost abolished on ice under steady-state conditions at 30 min (Table 7). Collectively, our assumptions are valid for anions.

For the estimation of $K_{p,uu,ss}$, ATP depletors such as rotenone were also used to stop the active uptake (Yamazaki et al., 1992); however, it is difficult to optimize experimental conditions for the exposure to ATP depletors to abolish the active uptake without affecting cell viability, and the effect of ATP depletion is often required to be insufficient to maintain viability (Yamazaki et al., 1993). Thus, this approach may lead to underestimation of $K_{p,uu,ss}$. The use of transporter inhibitors is another strategy to stop the active transport. However, before this, we should understand the major transport mechanism of the drugs to be tested, and confirm that the contribution of other transporters to the overall active uptake is negligible. In the case of statins, because Na^+-taurocholate cotransporting polypeptide (NTCP) is known to partly play a role in their hepatic uptake (Bi et al., 2013), the inhibition of NTCP in addition to OATPs is required; otherwise, insufficient inhibition of the hepatic uptake causes an underestimation of $K_{p,uu,ss}$.

In conclusion, $K_{p,uu}$ of statins were estimated in rat and human hepatocytes using two different methods based on steady-state uptake ($K_{p,uu,ss}$) and initial uptake rate ($K_{p,uu,v0}$). Considering the inside-negative membrane potential and subsequent asymmetrical diffusional clearance for influx and efflux, in theory, $K_{p,uu,ss}$ should be similar to true $K_{p,uu}$ ($K_{p,uu,true}$), whereas $K_{p,uu,V0}$ should be higher compared with $K_{p,uu,true}$. This can explain, at least in part, the discrepancies observed between $K_{p,uu,ss}$ and $K_{p,uu,V0}$ for statins in the present study. Using

the estimated $K_{p,uu}$ value and the ratio of diffusional uptake to active uptake determined in vitro, we can mathematically describe the relationship among permeation clearances across the sinusoidal membrane of hepatocytes, which can be applied for the construction of a physiologically-based pharmacokinetic model.

Although our current approach should be valid from the viewpoint of kinetic theory, we will need to practically validate our method for the *in vitro–in vivo* extrapolation of $K_{p,uu}$. One of the approaches is to compare the observed liver-to-blood total concentration ratio of positron emission tomography probes (e.g., [^{11}C]dehydropravastatin (Ijuin et al., 2012)) in humans with that predicted from experimentally estimated hepatic $K_{p,uu}$ and their unbound fractions in blood and hepatocytes. Another approach is to confirm whether the discrepancy of *in vitro* K_i values with regard to the medium concentration of inhibitors obtained with hepatocytes and recombinant enzymes can be well explained by *in vitro* $K_{p,uu}$ when target proteins are located inside the hepatocytes (e.g., inhibition of 3-hydroxy-3-methyl-glutaryl-coenzyme A reductase by statins, inhibition of metabolic enzymes and efflux transporters by inhibitor drugs). Such validations should strengthen our theoretical considerations for *in vitro* $K_{p,uu}$ estimation.

Authorship Contributions

Participated in research design: Yoshikado, Toshimoto, Nakada, Maeda, and Sugiyama.

Conducted experiments: Yoshikado, Nakada, and Ikejiri.

Performed data analysis: Yoshikado, Toshimoto, and Nakada.

Wrote or contributed to the writing of the manuscript: Yoshikado, Toshimoto, Nakada, Kusuhara, Maeda, and Sugiyama.

References

Baur H, Kasperek S, and Pfaff E (1975) Criteria of viability of isolated liver cells. *Hoppe Seylers Z Physiol Chem* **356:**827-838.

Bi YA, Qiu X, Rotter CJ, Kimoto E, Piotrowski M, Varma MV, Ei-Kattan AF, and Lai Y (2013) Quantitative assessment of the contribution of sodium-dependent taurocholate co-transporting polypeptide (NTCP) to the hepatic uptake of rosuvastatin, pitavastatin and fluvastatin. *Biopharm Drug Dispos* **34:**452-461.

Bradford NM, Hayes MR, and McGivan JD (1985) The use of 36Cl- to measure cell plasma membrane potential in isolated hepatocytes--effects of cyclic AMP and bicarbonate ions. *Biochim Biophys Acta* **845:**10-16.

Brown HS, Wilby AJ, Alder J, and Houston JB (2010) Comparative use of isolated hepatocytes and hepatic microsomes for cytochrome P450 inhibition studies: transporter-enzyme interplay. *Drug metabolism and disposition: the biological fate of chemicals* **38:**2139-2146.

Chu X, Korzekwa K, Elsby R, Fenner K, Galetin A, Lai Y, Matsson P, Moss A, Nagar S, Rosania GR, Bai JP, Polli JW, Sugiyama Y, Brouwer KL, and International Transporter C (2013) Intracellular drug concentrations and transporters: measurement, modeling, and implications for the liver. *Clin Pharmacol Ther* **94:**126-141.

Eaton DL and Klaassen CD (1978) Carrier-mediated transport of ouabain in isolated hepatocytes. *The Journal of pharmacology and experimental therapeutics* **205:**480-488.

Edmondson JW, Miller BA, and Lumeng L (1985) Effect of glucagon on hepatic taurocholate uptake: relationship to membrane potential. *Am J Physiol* **249:**G427-433.

Fitz JG and Scharschmidt BF (1987) Regulation of transmembrane electrical potential gradient in rat hepatocytes in situ. *Am J Physiol* **252:**G56-64.

Hallifax D and Houston JB (2006) Uptake and intracellular binding of lipophilic amine drugs by isolated rat hepatocytes and implications for prediction of in vivo metabolic clearance. *Drug metabolism and disposition: the biological fate of chemicals* **34:**1829-1836.

He J, Yu Y, Prasad B, Link J, Miyaoka RS, Chen X, and Unadkat JD (2014) PET imaging of Oatp-mediated hepatobiliary transport of [(11)C] rosuvastatin in the rat. *Molecular pharmaceutics* **11:**2745-2754.

Ichikawa M, Tsao SC, Lin TH, Miyauchi S, Sawada Y, Iga T, Hanano M, and Sugiyama Y (1992) 'Albumin-mediated transport phenomenon' observed for ligands with high membrane permeability. Effect of the unstirred water layer in the Disse's space of rat liver. *J Hepatol* **16:**38-49.

Iga T, Eaton DL, and Klaassen CD (1979) Uptake of unconjugated bilirubin by isolated rat hepatocytes. *Am J Physiol* **236:**C9-14.

Ijuin R, Takashima T, Watanabe Y, Sugiyama Y, and Suzuki M (2012) Synthesis of [(11)C]dehydropravastatin, a PET probe potentially useful for studying OATP1B1 and MRP2 transporters in the liver. *Bioorg Med Chem* **20:**3703-3709.

International Transporter C, Giacomini KM, Huang SM, Tweedie DJ, Benet LZ, Brouwer KL,

Chu X, Dahlin A, Evers R, Fischer V, Hillgren KM, Hoffmaster KA, Ishikawa T, Keppler D, Kim RB, Lee CA, Niemi M, Polli JW, Sugiyama Y, Swaan PW, Ware JA, Wright SH, Yee SW, Zamek-Gliszczynski MJ, and Zhang L (2010) Membrane transporters in drug development. *Nat Rev Drug Discov* **9:**215-236.

Kanduser M, Sentjurc M, and Miklavcic D (2008) The temperature effect during pulse application on cell membrane fluidity and permeabilization. *Bioelectrochemistry* **74:**52-57.

Kletzien RF, Pariza MW, Becker JE, and Potter VR (1975) A method using 3-O-methyl-D-glucose and phloretin for the determination of intracellular water space of cells in monolayer culture. *Anal Biochem* **68:**537-544.

Kristensen LO and Folke M (1984) Volume-regulatory K+ efflux during concentrative uptake of alanine in isolated rat hepatocytes. *Biochem J* **221:**265-268.

Lundquist P, Englund G, Skogastierna C, Loof J, Johansson J, Hoogstraate J, Afzelius L, and Andersson TB (2014) Functional ATP-binding cassette drug efflux transporters in isolated human and rat hepatocytes significantly affect assessment of drug disposition. *Drug metabolism and disposition: the biological fate of chemicals* **42:**448-458.

Miyauchi S, Sawada Y, Iga T, Hanano M, and Sugiyama Y (1993) Comparison of the hepatic uptake clearances of fifteen drugs with a wide range of membrane permeabilities in isolated rat hepatocytes and perfused rat livers. *Pharmaceutical research* **10:**434-440.

Neuhoff S, Ungell AL, Zamora I, and Artursson P (2003) pH-dependent bidirectional transport of weakly basic drugs across Caco-2 monolayers: implications for drug-drug

interactions. *Pharmaceutical research* **20:**1141-1148.

Nezasa K, Higaki K, Takeuchi M, Nakano M, and Koike M (2003) Uptake of rosuvastatin by isolated rat hepatocytes: comparison with pravastatin. *Xenobiotica* **33:**379-388.

Nezasa K, Takao A, Kimura K, Takaichi M, Inazawa K, and Koike M (2002) Pharmacokinetics and disposition of rosuvastatin, a new 3-hydroxy-3-methylglutaryl coenzyme A reductase inhibitor, in rat. *Xenobiotica* **32:**715-727.

Niemi M, Pasanen MK, and Neuvonen PJ (2011) Organic anion transporting polypeptide 1B1: a genetically polymorphic transporter of major importance for hepatic drug uptake. *Pharmacological reviews* **63:**157-181.

Reinoso RF, Telfer BA, Brennan BS, and Rowland M (2001) Uptake of teicoplanin by isolated rat hepatocytes: comparison with in vivo hepatic distribution. *Drug metabolism and disposition: the biological fate of chemicals* **29:**453-459.

Saito S, Murakami Y, Miyauchi S, and Kamo N (1992) Measurement of plasma membrane potential in isolated rat hepatocytes using the lipophilic cation, tetraphenylphosphonium: correction of probe intracellular binding and mitochondrial accumulation. *Biochim Biophys Acta* **1111:**221-230.

Schirris TJ, Ritschel T, Bilos A, Smeitink JA, and Russel FG (2015) Statin Lactonization by Uridine 5'-Diphospho-glucuronosyltransferases (UGTs). *Mol Pharm* **12:**4048-4055.

Shitara Y, Maeda K, Ikejiri K, Yoshida K, Horie T, and Sugiyama Y (2013) Clinical significance of organic anion transporting polypeptides (OATPs) in drug disposition: their roles in hepatic clearance and intestinal absorption. *Biopharm Drug Dispos*

34:45-78.

Shitara Y and Sugiyama Y (2006) Pharmacokinetic and pharmacodynamic alterations of 3-hydroxy-3-methylglutaryl coenzyme A (HMG-CoA) reductase inhibitors: drug-drug interactions and interindividual differences in transporter and metabolic enzyme functions. *Pharmacol Ther* **112:**71-105.

Shugarts S and Benet LZ (2009) The role of transporters in the pharmacokinetics of orally administered drugs. *Pharmaceutical research* **26:**2039-2054.

Smith DA, Di L, and Kerns EH (2010) The effect of plasma protein binding on in vivo efficacy: misconceptions in drug discovery. *Nat Rev Drug Discov* **9:**929-939.

Smith NF, Figg WD, and Sparreboom A (2005) Role of the liver-specific transporters OATP1B1 and OATP1B3 in governing drug elimination. *Expert opinion on drug metabolism & toxicology* **1:**429-445.

Sugano K, Kansy M, Artursson P, Avdeef A, Bendels S, Di L, Ecker GF, Faller B, Fischer H, Gerebtzoff G, Lennernaes H, and Senner F (2010) Coexistence of passive and carrier-mediated processes in drug transport. *Nat Rev Drug Discov* **9:**597-614.

Weinman SA, Graf J, and Boyer JL (1989) Voltage-driven, taurocholate-dependent secretion in isolated hepatocyte couplets. *Am J Physiol* **256:**G826-832.

Wondergem R and Castillo LB (1988) Quinine decreases hepatocyte transmembrane potential and inhibits amino acid transport. *Am J Physiol* **254:**G795-801.

Yabe Y, Galetin A, and Houston JB (2011) Kinetic characterization of rat hepatic uptake of 16 actively transported drugs. *Drug Metab Dispos* **39:**1808-1814.

Yamazaki M, Suzuki H, Hanano M, Tokui T, Komai T, and Sugiyama Y (1993) Na(+)-independent multispecific anion transporter mediates active transport of pravastatin into rat liver. *Am J Physiol* **264:**G36-44.

Yamazaki M, Suzuki H, Sugiyama Y, Iga T, and Hanano M (1992) Uptake of organic anions by isolated rat hepatocytes. A classification in terms of ATP-dependency. *J Hepatol* **14:**41-47.

Yoshikado T, Yoshida K, Kotani N, Nakada T, Asaumi R, Toshimoto K, Maeda K, Kusuhara H, and Sugiyama Y (2016) Quantitative Analyses of Hepatic OATP-Mediated Interactions Between Statins and Inhibitors Using PBPK Modeling With a Parameter Optimization Method. *Clinical pharmacology and therapeutics* **100:**513-523.

Footnotes

TY, KT, and TN contributed to the research equally. This work was financially supported by Grant-in-Aid for Scientific Research (S) and the Scientific Research on Innovative Areas HD-Physiology from the Ministry of Education, Culture, Sports, Sciences, and Technology in Japan [Grants 24229002, 23136101].

Figure Legends

Figure 1. Uptake of diazepam (1 μM; A), pitavastatin (1 μM; B), rosuvastatin (1 μM; C), and pravastatin (1 μM; D) by rat hepatocytes measured after incubation at 37°C for 0.5–30 min. The data are presented as mean + standard deviation (SD) (n = 3).

Figure 2. Uptake of diazepam (1 μM; A and E), pitavastatin (1 μM; B and F), rosuvastatin (1 μM; C and G), and pravastatin (1 μM; D and H) by human hepatocytes measured after incubation at 37°C for 0.5–60 min. (A–D) Cryopreserved human hepatocytes from a single donor (Lot. Hu8075) were used. (E–H) Pooled cryopreserved human hepatocytes from 20 mixed-sex donors (Lot. TFF) were used. The data are presented as mean + SD (n = 3).

Figure 3. Comparison of $K_{p,uu}$ and $f_{T,cell}$ for three statins in rat and human hepatocytes obtained by two different methods. (A, C) $K_{p,uu,V0}$ and $f_{T,cell,V0}$ in rat hepatocytes derived from a previous report (Yabe et al., 2011) are plotted against $K_{p,uu,ss}$ and $f_{T,cell,ss}$ obtained in the present study as closed symbols. $K_{p,uu,V0}$ and $f_{T,cell,V0}$ obtained in the present study are plotted against $K_{p,uu,ss}$ and $f_{T,cell,ss}$ as open symbols. (B, D) $K_{p,uu,V0}$ and $f_{T,cell,V0}$ in human hepatocytes from a single donor (Lot. Hu8075) are plotted against $K_{p,uu,ss}$ and $f_{T,cell,ss}$ obtained in the present study as gray symbols. $K_{p,uu,V0}$ and $f_{T,cell,V0}$ in pooled human hepatocytes from 20 -gender donors (Lot. TFF) are plotted against $K_{p,uu,ss}$ and $f_{T,cell,ss}$ as open symbols. 1: pitavastatin, 2: rosuvastatin, 3: pravastatin. Solid and dashed lines denote unity and 3-fold boundaries, respectively. The data are presented as mean + SD for the X- and Y-axis (n = 3).

Figure 4. Uptake of TPP^+ by human hepatocytes measured after incubation at 37°C (circles) or on ice (triangles) for 0.5–60 min. Hepatocytes were incubated with 3 μM TPP^+ (closed

symbols) or both 3 μM TPP^+ and 20 μM amphotericin B (open symbols). Pooled cryopreserved human hepatocytes from 50 mixed-sex donors (Lot. HUE50C) were used. The data are presented as mean + SD (n = 3).

Figure 5. Theoretical simulation of $K_{p,uu,ss}/K_{p,uu,true}$ (=$R_{ss/true}$: blue) and $K_{p,uu,V0}/K_{p,uu,true}$ (=$R_{V0/true}$: red) using Equations 12 and 13. (A) The solid line represents the simulation result for pitavastatin. (B) The broken line represents simulation results for rosuvastatin and pravastatin. Arrows represent the λ for statins estimated from our experiments with Caco-2 cells.

Figure 6. Comparison of $K_{p,uu,ss,corrected}$ and $K_{p,uu,V0,corrected}$ corrected by Equations 14 and 15 using $R_{ss/true}$ and $R_{V0/true}$ (Table 8). (A) Closed symbols: original $K_{p,uu,V0}$ in rat hepatocytes were obtained from a previous report (Yabe et al., 2011). Open symbols: original $K_{p,uu,V0}$ values were obtained in the present study. (B) Gray symbols: original $K_{p,uu,V0}$ values were obtained in human hepatocytes from a single donor (Lot. Hu8075). Open symbols: original $K_{p,uu,V0}$ values were obtained in pooled human hepatocytes from 20 mixed-sex donors (Lot. TFF). 1: pitavastatin, 2: rosuvastatin, 3: pravastatin. Solid and dashed lines denote unity and 3-fold boundaries, respectively. The data are presented as mean + SD for the X- and Y-axis (n = 3).

Table 1

Determination of λ based on the pH-dependent permeation data of statins observed in Caco-2 cells.

Drug	$f_{i,ion}$ [a]	$f_{i,uion}$ [a]	$f_{o,ion}$ [a]	$f_{o,uion}$ [a]	pKa [b]	$PS_{dif,inf,uion,Caco-2}$ [c]	λ [c]
						$\times 10^{-6}$ μL/min/well	
Pitavastatin	0.857	0.143	0.905	0.095	4.46	3487 ± 1403	0.0282 ± 0.0204
Rosuvastatin	0.986	0.014	0.991	0.009	4.6	714 ± 68	0.0112 ± 0.0035
Pravastatin	0.986	0.014	0.991	0.009	4.6	111 ± 19	0.188 ± 0.038

Values are shown as the mean ± SD.

[a] The $f_{i,ion}$ and $f_{o,ion}$ were calculated based on Henderson-Hasselbalch equation assuming that intracellular pH and medium pH are 7.2 and 7.4, respectively. The $f_{i,uion}$ and $f_{o,uion}$ were subtracted $f_{i,ion}$ and $f_{o,ion}$ from one, respectively.

[b] Fixed at values obtained from the manufacturer's Interview Forms.

[c] The $PS_{dif,inf,uion,Caco-2}$ and λ were determined by fitting Equation 9 to the pH-dependent permeation data of statins observed in Caco-2 cells (Supplemental Figure 1).

Table 2

$K_{p,uu,ss}$ and $f_{T,cell,ss}$ in rat hepatocytes.

Drug	C/M ratio [a]		$K_{p,uu,ss}$ [b]	$f_{T,cell,ss}$ [b]
	37°C	On ice		
Diazepam	58.9 ± 7.3	69.3 ± 9.7	0.851 ± 0.024	0.0147 ± 0.0022
Pitavastatin	324 ± 174	29.6 ± 11.5	10.8 ± 4.4	0.0381 ± 0.0167
Rosuvastatin	78.1 ± 37.1	7.80 ± 4.07	13.1 ± 7.7	0.149 ± 0.060
Pravastatin	12.5 ± 7.7	1.80 ± 0.56	6.69 ± 2.76	0.600 ± 0.217

Values are shown as the mean ± SD (n = 3).

[a] C/M ratios were calculated using the uptake data at 30 min (Fig. 1).

[b] The $K_{p,uu,ss}$ and $f_{T,cell,ss}$ were calculated from C/M ratios using Equations 2 and 3, respectively.

Table 3

Kinetic parameters for the initial uptake rates of pitavastatin, rosuvastatin, and pravastatin in rat hepatocytes.

Drug	V_{max} [a]	K_m [a]	V_{max}/K_m	PS_{dif} [a]	$K_{p,uu,V0}$ [b]	$f_{T,cell,V0}$ [b]
	pmol/min/10^6 cells	*μM*	*μL/min/10^6 cells*	*μL/min/10^6 cells*		
Pitavastatin	893± 124	5.43 ± 1.29	164 ± 45	3.00 ± 1.41	55.8 ± 29.9	0.172 ± 0.131
Rosuvastatin	250 ± 80	2.86 ± 1.82	87.4 ± 62.3	1.76 ± 1.15	50.7 ± 48.0	0.649 ± 0.688
Pravastatin	178 ± 11	20.3 ± 1.4	8.77 ± 0.81	1.16 ± 0.08	8.56 ± 0.87	0.685 ± 0.428

Values are shown as the mean ± SD.

[a] The initial uptake rate in rat hepatocytes was calculated from the uptake of [^{3}H]pitavastatin, [^{3}H]rosuvastatin, and [^{3}H]pravastatin for 0.5–1.5 min. Kinetic parameters are obtained by fitting to the data at 7 concentrations (0.1, 0.3, 1, 3, 10, 30, and 100 μM for all statins; Supplemental Figure 2) using Equation 4.

[b] The $K_{p,uu,V0}$ and $f_{T,cell,V0}$ were calculated using Equations 5 and 6, respectively. C/M ratios at 37°C (Table 2) were used for the calculation of the $f_{T,cell,V0}$.

Table 4

$K_{p,uu,ss}$ and $f_{T,cell,ss}$ in human hepatocytes.

Drug	Lot	C/M ratio [c]		$K_{p,uu,ss}$ [d]	$f_{T,cell,ss}$ [d]
		37°C	On ice		
Diazepam	Hu8075 [a]	216 ± 20	181 ± 38	1.19 ± 0.51	0.00553 ± 0.00115
	TFF [b]	124 ± 53	303 ± 22	0.409 ± 0.247	0.00330 ± 0.00024
Pitavastatin	Hu8075 [a]	471 ± 88	35.2 ± 2.6	13.4 ± 2.7	0.0284 ± 0.0021
	TFF [b]	150 ± 2.6	21.8 ± 3.2	6.92 ± 1.02	0.0460 ± 0.0068
Rosuvastatin	Hu8075 [a]	52.2 ± 8.6	4.51 ± 0.41	11.6 ± 2.2	0.222 ± 0.020
	TFF [b]	27.2 ± 2.5	4.28 ± 0.53	6.36 ± 1.06	0.234 ± 0.029
Pravastatin	Hu8075 [a]	3.73 ± 0.73	1.84 ± 0.12	2.03 ± 0.54	0.545 ± 0.035
	TFF [b]	2.65 ± 1.29	2.07 ± 0.64	1.28 ± 0.89	0.484 ± 0.151

Values are shown as the mean ± SD (n = 3).

[a] Isolated cryopreserved human hepatocytes (Lot. Hu8075) were incubated with diazepam (0.2 μM), pitavastatin (0.1 μM), rosuvastatin (0.1 μM) and pravastatin (0.2 μM).

[b] Pooled cryopreserved human hepatocytes from 20 mixed-sex donors (Lot. TFF) were incubated with diazepam (1 µM), pitavastatin (0.5 µM), rosuvastatin (0.5 µM) and pravastatin (1 µM).

[c] C/M ratios at 37°C and on ice were calculated using the uptake data at 30 min and 60 min, respectively (Fig. 2).

[d] The $K_{p,uu,ss}$ and $f_{T,cell,ss}$ were calculated from C/M ratios using Equations 2 and 3, respectively.

Table 5

Kinetic parameters for the initial uptake of pitavastatin, rosuvastatin, and pravastatin in human hepatocytes.

Drug	Lot	V_{max}	K_m	V_{max}/K_m	PS_{dif}	$K_{p,uu,V0}$ [d]	$f_{T,cell,V0}$ [d]
		pmol/min/10^6 cells	*μM*	*$\mu L/min/10^6$ cells*	*$\mu L/min/10^6$ cells*		
Pitavastatin	Hu8075 [a]	403 ± 84	4.77 ± 1.80	84.5 ± 36.4	0.388 ± 0.912	219 ± 521	0.465 ± 1.110
	TFF [b]	148 ± 66.1	1.78 ± 1.04	83.1 ± 61.1	4.36 ± 0.70	20.1 ± 14.4	0.134 ± 0.096
Rosuvastatin	Hu8075 [a]	198 ± 50	21.5 ± 7.8	9.21 ± 4.07	0.0462 ± 0.1547	200 ± 673	3.83 ± 12.91
	TFF [b]	23.0 ± 8.6	4.49 ± 1.72	5.12 ± 2.75	2.07 ± 0.279	3.47 ± 1.41	0.128 ± 0.053
Pravastatin	Hu8075 [a]	93.8 ± 56.0	127 ± 81	0.739 ± 0.645	0.0137 ± 0.0922	54.8 ± 363.7	14.7 ± 97.5
	TFF	Not determined [c]					

Values are shown as the mean ± SD.

[a] The initial uptake rate in isolated cryopreserved human hepatocytes (Lot. Hu8075) was calculated from the uptake of [^{3}H]pitavastatin, [^{3}H]rosuvastatin, and [^{3}H]pravastatin for 0.5–2.0 min. Kinetic parameters are obtained by fitting to the data at several concentrations (0.1, 0.3, 1, 3, 10, 30, and 100 μM for pitavastatin; 0.1, 0.3, 1,3, 10, 30, and 300 μM for rosuvastatin; 1, 3, 100, and 300 μM for pravastatin; Supplemental Figure 3A-C) using Equation 4.

[b] The initial uptake rate in pooled cryopreserved human hepatocytes from 20 mixed-sex donors (Lot. TFF) was calculated from the uptake of [^{3}H]pitavastatin and [^{3}H]rosuvastatin for 0.5–1.5 min. Kinetic parameters are obtained by fitting to the data at several concentrations (0.1, 0.3, 1, 3, 10, 30, and 100 μM for pitavastatin; 0.1, 0.3, 1,3, 10, 30, and 300 μM for rosuvastatin; Supplemental Figure 3D, E) using Equation 4.

[c] Not determined in Lot. TFF because a concentration (0.5-300 μM)-dependent saturation of the uptake of pravastatin was not observed clearly.

[d] The $K_{p,uu,V0}$ and $f_{T,cell,V0}$ were calculated using Equations 5 and 6, respectively. C/M ratios at 37°C (Table 4) were used for the calculation of the $f_{T,cell,V0}$.

Table 6

$f_{T,homogenate}$ in human liver homogenate.

Drug	$f_{T,homogenate}$		
	37ºC	On ice	37ºC/On ice ratio
Diazepam	0.0259 ± 0.0018	0.0242 ± 0.0016	1.07 ± 0.10
Pitavastatin	0.0301 ± 0.0017	0.0344 ± 0.0018	0.875 ± 0.067
Rosuvastatin	0.237 ± 0.037	0.206 ± 0.025	1.15 ± 0.23
Pravastatin	0.183 ± 0.022	0.167 ± 0.020	1.10 ± 0.19

Values are shown as the mean ± SD (n = 3).

Table 7

Theoretical calculation of the membrane potential (ΔΨ) using the measured C/M ratios of TPP^+.

Temparature	C/M ratio		$\Delta\Psi$ [a]	Φ [a]
	-AMB	+AMB	*mV*	
37°C	442.7 ± 31.1	142.4 ± 4.3	-30.22 ± 2.04	3.109 ± 0.237
On ice	9.5 ± 1.4	11.3 ± 0.5	4.97 ± 4.12	0.840 ± 0.128

Values are shown as the mean ± SD (n = 4).

[a] ΔΨ and Φ were calculated using Equations 10 and S5, respectively.

Table 8

Theoretical calculation of $K_{p,uu,true}$, $K_{p,uu,V0}$, and $K_{p,uu,ss}$ using the calculated membrane potential.

Drug	Lot	$K_{p,uu,true}$ [b]	$K_{p,uu,V0}$ [b]	$K_{p,uu,ss}$ [b]	$R_{V0/true}$ [c]	$R_{ss/true}$ [c]
Pitavastatin	Hu8075	90.7	198	106	2.18	1.17
	TFF	8.35	18.3	9.75	2.18	1.17
Rosuvastatin	Hu8075	72.4	199	71.9	2.74	0.994
	TFF	1.26	3.45	1.25	2.74	0.994
Pravastatin	Hu8075	17.9	54.5	15.2	3.05	0.850
	TFF	Not calculated [d]				

Values are shown as the mean ± SD (n = 4).

[b] Theoretical values of $K_{p,uu,true}$, $K_{p,uu,V0}$, and $K_{p,uu,ss}$ were calculated by Equations S6, S8, and S11, respectively. The $f_{i,ion}$, $f_{o,ion}$, $f_{i,uion}$, $f_{o,uion}$, λ (Table 1), V_{max}/K_m (Table 5), $PS_{dif,inf,uion}$ in each lot of human hepatocytes determined by $f_{o,ion}$, $f_{o,uion}$, λ and PS_{dif} (Table 5) according to Equation 7 were used for the calculation.

[c] $R_{V0/true} = K_{p,uu,V0} / K_{p,uu,true}$ and $R_{ss/true} = K_{p,uu,ss} / K_{p,uu,true}$ were calculated by Equations 11 and 12.

[d] Not calculated for Lot. TFF because kinetic parameters (K_m, V_{max} and PS_{dif}) of pravastatin were not determined (Table 5).

DMD Fast Forward. Published on May 3, 2017 as DOI: 10.1124/dmd.116.074823
This article has not been copyedited and formatted. The final version may differ from this version.

Figure 1

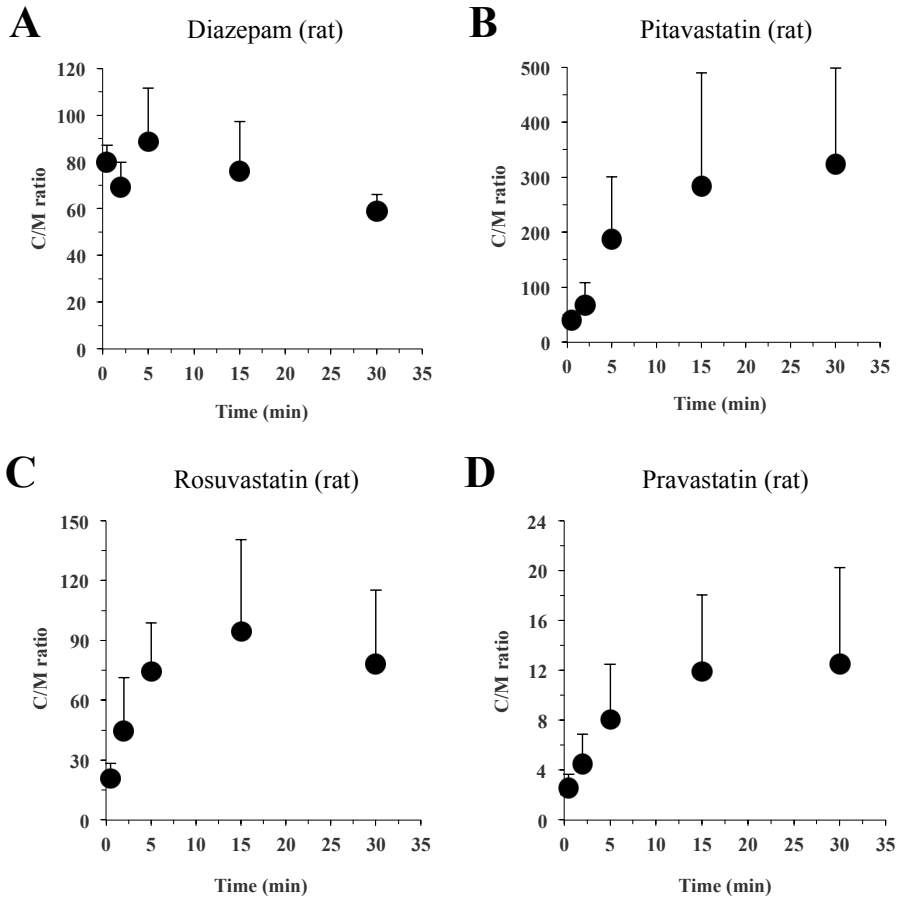

DMD Fast Forward. Published on May 3, 2017 as DOI: 10.1124/dmd.116.074823
This article has not been copyedited and formatted. The final version may differ from this version.

Figure 2

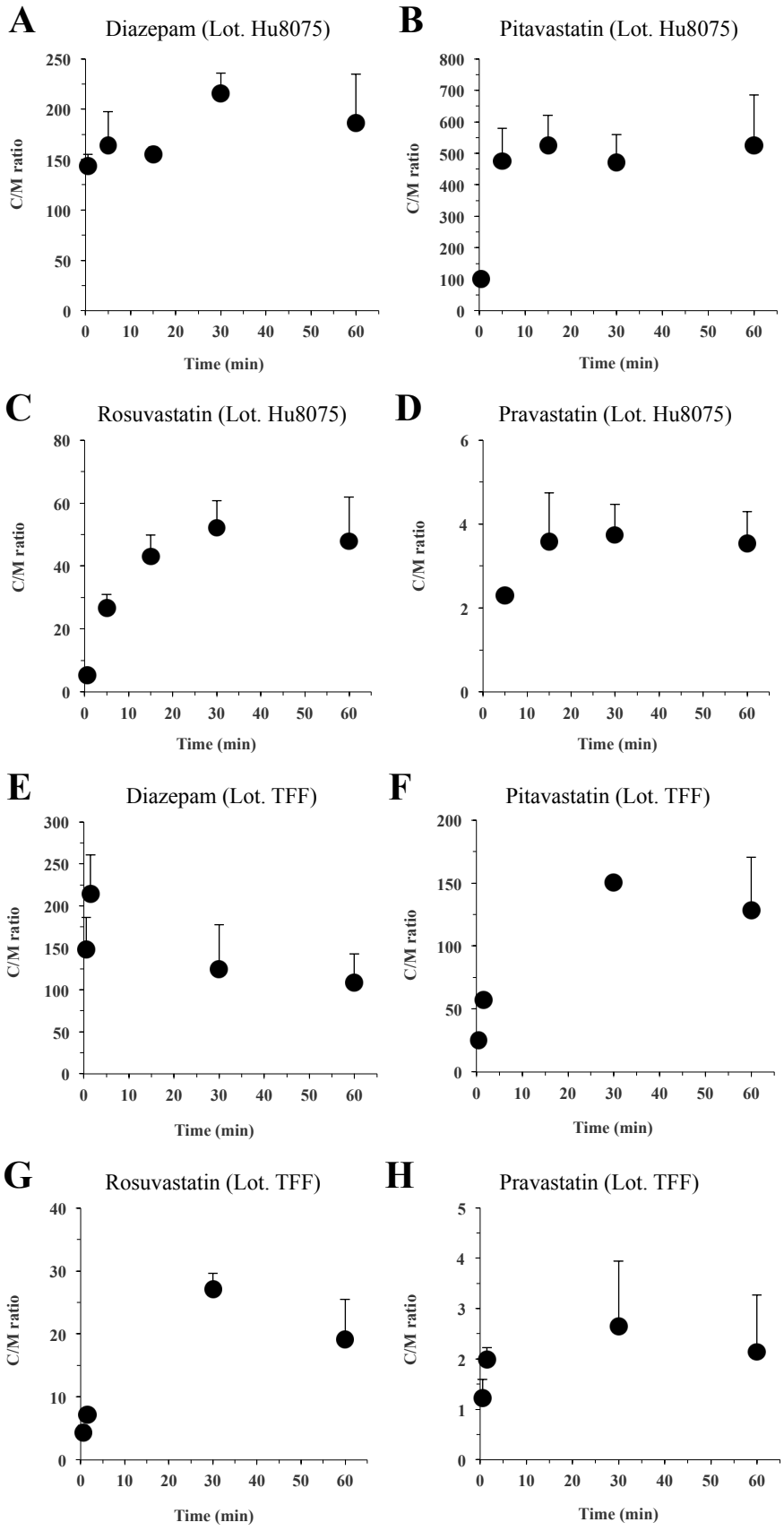

Figure 3

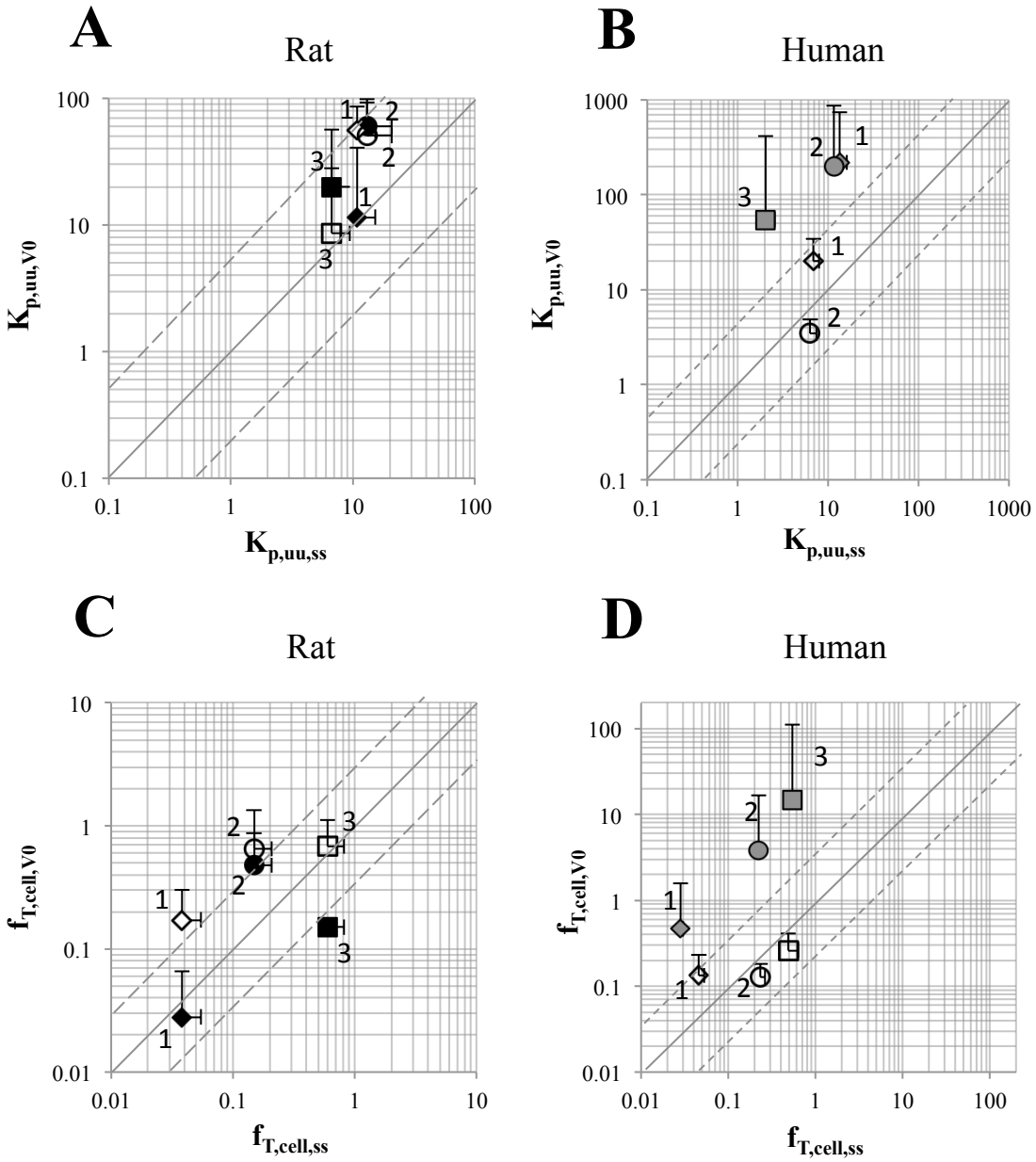
A
Rat
B
Human
C
Rat
D
Human
$K_{p,uu,V0}$
$K_{p,uu,ss}$
$f_{T,cell,V0}$
$f_{T,cell,ss}$
0.01
0.1
1
10
100
1000

Figure 4

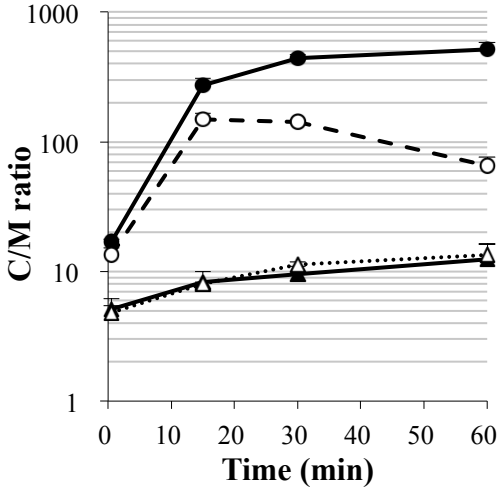

Figure 5

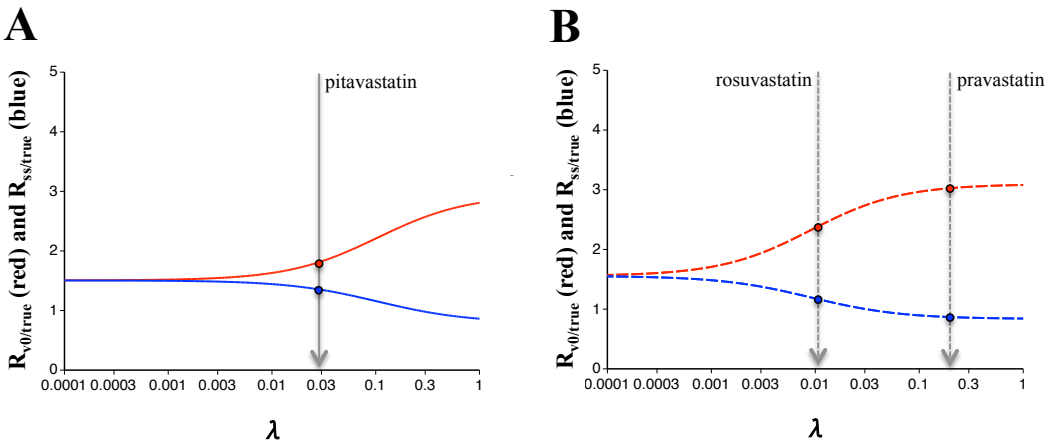
A
B
pitavastatin
rosuvastatin
pravastatin
$R_{v0/true}$ (red) and $R_{ss/true}$ (blue)
0
1
2
3
4
5
0.0001 0.0003 0.001 0.003 0.01 0.03 0.1 0.3 1
λ

Figure 6

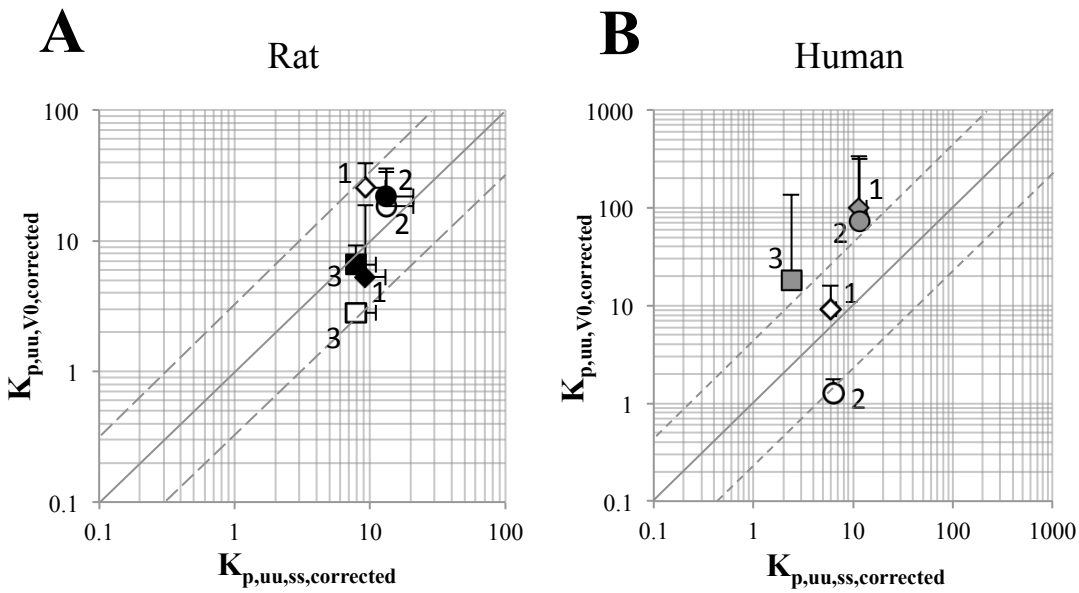
A
Rat
B
Human
100
10
1
0.1
1000
0.1
1
10
100
1000
$K_{p,uu,V0,corrected}$
$K_{p,uu,ss,corrected}$
1
2
3